Recent progress in polydiacetylene mechanochromism

Bratati Das, Seiko Jo, Jianlu Zheng, Jiali Chen, Kaori Sugihara*

Polydiacetylenes (PDAs) are a family of mechanochromic polymers that change color from blue to red and emit fluorescence when exposed to external stimuli, making them extremely popular materials in biosensing. Although several informative reviews on PDA biosensing have been reported in the last few years, their mechanochromism, where external forces induce the color transition, has not been reviewed for a long time. This minireview summarizes recent progress in PDA mechanochromism, with a special focus on the quantitative and nanoscopic data that have emerged in recent years.

1. Introduction

Mechanochromic polymer polydiacetylenes (PDAs) have garnered attention owing to their unique force-sensing mechanism that can be used to detect forces impossible to quantify by the conventional technique such as piezoresistive[1, 2] or capacitive tactile sensors,[3, 4] and their potential for applications in chemo/biosensing. They were first reported by Wegner in 1969.[5] Their mechanosensitive conjugated backbone with customizable side chains reacts to a specific type of external perturbation, which turns their original blue color to red and causes them to fluoresce. They are frequently fabricated using lipidic monomers, where a polar group is attached on one side of the carbon chains, which then self-assemble into vesicles,[6, 7] supported bilayers,[8, 9] and monolayers.[10] Upon ultraviolet (UV) irradiation, they polymerize into PDA (Figure 1).

Many papers have been published in the past few decades, where researchers have attempted to use PDAs as chromic and fluorescence sensors for the detection of temperature,[11] pH changes,[12] mechanical stimuli,[13] ions,[14] solvents,[15] light,[16] surfactants,[17] bacteria,[18] and other biomolecules[19] such as peptides,[20, 21] as well as for other non-sensing applications.[22-31] Significant progress has been made to improve their specificity by synthesizing monomers with different headgroups.[32-34] For example, a PDA with an epoxy headgroup was shown to present selectivity toward mercury(II).[32] The recent introduction of a differential approach, in which the color change of several types of PDAs was used as a fingerprint to identify solvents,[15] has further improved their selectivity. These promising results have paved the way for overcoming the rather weak specificity of PDAs and the development of a convenient colorimetric sensor.

Institute of Industrial Science, The University of Tokyo, 4-6-1 Komaba Meguro-Ku, Tokyo 153-8505, Japan

The mechanochromic properties of PDAs have been extensively characterized by the Langmuir–Blodgett technique,[35] electron paramagnetic resonance (EPR),[36] X-ray crystallography,[37] ultraviolet-visible (UV-vis) spectroscopy,[38] fluorescence,[20] infrared (IR) spectroscopy,[39] Raman spectroscopy,[40] nuclear magnetic resonance (NMR),[41] scanning tunneling microscopy (STM),[42] atomic force microscopy (AFM),[43] fluorescence microscopy,[44] and electrical conductivity measurements.[45] These experimental efforts, combined with theoretical works,[46] have provided a mechanistic model where the torsion of the sidechains shortens the π conjugation in the backbone, thus broadening the bandgap to cause a blueshift in the absorption.

Despite our general understanding of their mechanism and the large number of reports in biosensing, the lack of a quantitative understanding of the color-changing mechanism of PDAs at the nanoscale has hindered further development until recently, when AFM was introduced.[44, 47, 48] The recent technological advancement of AFM could shift PDA status as a quantitative mechanosensor at nanoscale, which may lead to another leap in the application development. Although there have been many informative reviews on PDAs, especially from the perspective of biosensing,[49-59] their mechanochromism, where external forces stimulate the blue-to-red transition, has not been reviewed since a brief report by Burns et al. in 2004.[60] In this minireview, therefore, we summarize the recent progress in PDA mechanosensing.

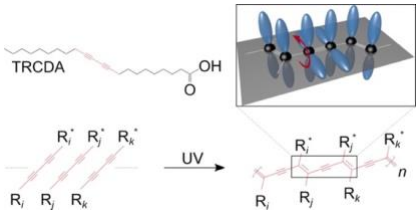

Figure 1: Chemical structure of 10,12-Tricosadiynoic acid (TRCDA) monomers, their polymerization by UV light, and a 3D scheme, where the p-orbitals of the carbon atoms (black) are colored in blue. This figure has been reproduced from ref [61] with permission from American Chemical Society, copyright 2020.

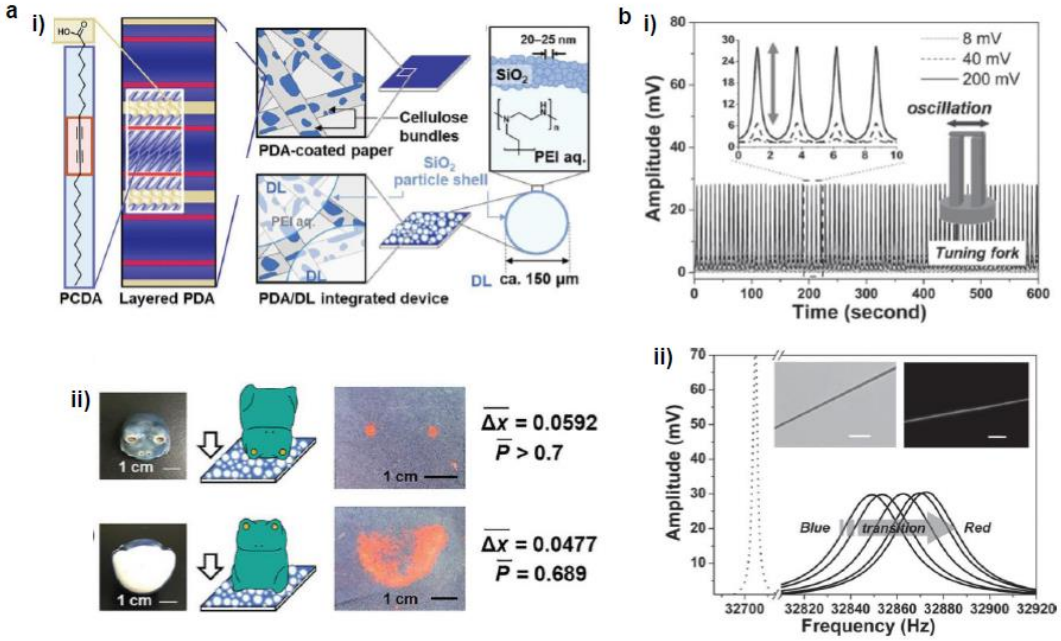

Figure 2: a, (i) Schematic illustrations of PDA/dry liquid-integrated paper device. (ii) Two different settings, where compression stresses were applied using a ceramic frog ornament. **b,** Hybrid mechanoresponsive polymer wire fabricated by mixing 10,12-pentacosadiynoic acid and a poly(ethylene oxide) matrix. (i) Time evolution of applied AC voltage, which vibrated the tuning fork to produce force pulse stimulus. ii) Oscillation amplitude vs. frequency curves shows the transduction process from the blue phase to the red phase. The inset shows bright-field and fluorescence images of the hybrid wire. Panel (a) has been adapted from ref [62] with permission from Wiley Online Library, copyright 2021. Panel (b) has been adapted from ref [63] with permission from Wiley Online Library, copyright 2013.

2. Polydiacetylene mechanosensing

2.1 Surface pressure

Tomioka et al.[10] investigated the dependence of the excitonic absorption on the surface pressure by observing the in situ reflection spectra of a PDA made of poly-(heptacosa-10,12-diynoic acid) at a N_2 gas–water interface. A reversible color change was observed when the PDA monolayer was compressed using a Langmuir–Blodgett trough at pressures between 3 and 25 mN m^{-1}. This reversible color change was reproducible after several cycles of compression and re-expansion. The fact that thermochromically irreversible poly-(heptacosa-10,12-diynoic acid) presented the reversibility in its mechanochromism indicates that the type of stimuli or the assembled polymer structure also affect the PDA reversibility.

2.2 Tensile strain

Reversible tensile strain (stretch)-induced phase transitions were observed by Nallicheri et al.[13] in segmented polyurethanes containing a small fraction of PDAs made of 2,4-hexadiyne-l,6-diol and 5,7-dodecadiyne-1,12-diol in hard-segmented structures. Polyurethanes (PUs) are a class of segmented copolymers composed of soft and hard segments. The diacetylene groups were linked to hard segments via a chain extender. When the strain levels were greater than 250%, irreversible hard-domain disruption was observed. From visible absorption spectroscopy, it was confirmed that during tensile elongation, stress was transmitted from the soft segments to the hard domains, where the hard segments were oriented perpendicular to the stretch direction. This resulted in a tensile (or shear) stress on PDAs oriented along the stretch direction, causing the color transformation.

2.3 Compression

Nakamitsu et al.[64] prepared a highly sensitive compression stress sensor by integrating a stimuli-responsive layered PDA and dry liquid (DL) on a filter paper substrate to induce a “response cascade” (Figure 2a). Macroscopic compression stresses induced the collapse of the DLs, which were micrometer-sized particles that consisted of liquid droplets covered by solid powders, starting the response cascade. As a consequence, the DLs released their interior liquid**,** a polyethyleneimine (PEI) solution, in response to mechanical stress. The subsequent PEI–PDA interaction induced color changes in the layered PDA. As the strength and duration of the compression increased, the intensity of the red color was enhanced. This compression stress sensor visualized weak compression stresses on the order of 3.9 Pa–4.9 kPa, comparable to those upon the impact of an object. The device has the potential for the visualization and measurement of weak mechanical stresses in biomedical and healthcare fields.

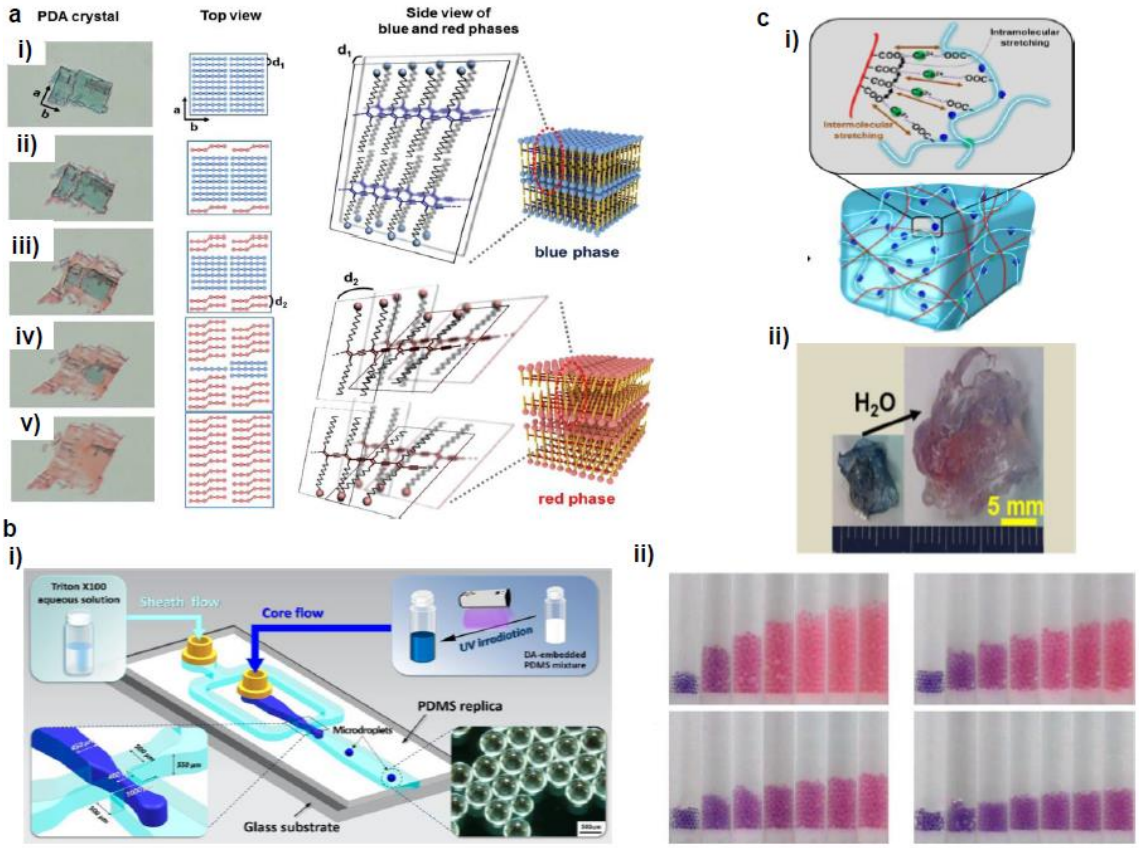

Figure 3: a, PDA microcrystal embedded in PDMS experienced drastic color and shape changes during PDMS swelling in octane at i) 0, ii) 5, iii) 10, iv) 15, and v) 23 min. **b**, Schematic diagram of a microfluidic chip used for the generation of PDA-embedded PDMS microdroplets and an optical microscopic image of the microdroplets. ii) Photographs of tubes that contain PDA-embedded PDMS microbeads upon exposure to pentane (upper left), heptane (upper right), nonane (lower left), and undecane (lower right). **c**, i) Schematic diagram of alginate hydrogel-assisted PDA and ii) its colorimetric response upon water absorption. Panel (a) has been adapted from ref [65] with permission from Wiley Online Library, copyright 2014. Panel (b) has been adapted from ref [66] with permission from American Chemical Society, copyright 2015. Panels (c) has been adapted from ref [67] with permission from American Chemical Society, copyright 2015.

2.4 Shear

Lee et al.[68] examined the shear-induced color transition of PDA vesicles in polymeric solutions made of 2% poly(vinyl alcohol) + 1% sodium borate (PVA/B), 15% PVA and 1% hyaluronic acid (HA) dissolved in water using a rheometer. In the PVA/B solution at 47 °C, shear at 100 Pa was sufficient to induce a blue–red transition in PDA vesicles made of 10,12-pentacosadiynoic acid (PCDA). In contrast, there was no color change in the PVA or HA solutions. The authors interpreted the color change as a result of the alteration of the structure of the PDA polymeric backbone owing to perturbation. However, the experimental setup used was not able to distinguish the effect of the shear and the increased temperature owing to the mixing, which made it difficult to conclude whether the shear itself induced the color change.

2.5 Oscillation

Feng et al.[63] fabricated a hybrid mechanoresponsive polymer wire by mixing PDA made of 10,12-pentacosadiynoic acid into poly(ethylene oxide) (PEO) as a polymer matrix (Figure 2b). The color change was induced by high-frequency mechanical oscillations controlled by AC voltages. The efficiency of the color transition increased by decreasing the diameter of the wires, because smaller diameters minimize the defect density and thus improve the mechanical transduction. This process was characterized using Raman spectroscopy and the resonant frequency shifts of the hybrid wire. Such a combination of cost-effective, easily processable polymers with PDA may be useful as a force sensor for detecting stresses and damages at the microscale.

2.6 Swelling

Park et al.[65] developed a PDA–polydimethylsiloxane (PDMS) composite sensor, which underwent a blue-to-red colorimetric transition during swelling upon exposure to different solvents (Figure 3a). The composite sensor was easy to fabricate by the

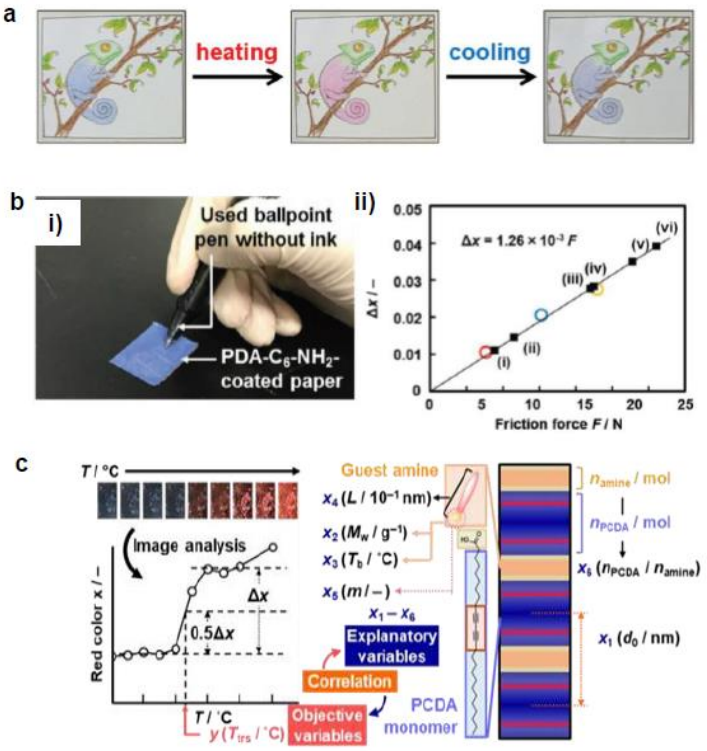

Figure 4: a, A hand-writable PDA sensor by using mixing–molding polymerization process. Drawings based on these pens responded to heating, cooling, and rubbing. **b**, (i) PDA-C6-NH_2-coated paper was tested against writing pressure. (ii) The intensity of the red color (Δx) vs. the applied friction force. **c**, (i) Sparse modeling toward the prediction of color-transition temperatures based on the sample image analysis. Panel (a) has been adapted from ref [69] with permission from Wiley Online Library, copyright 2016. Panel (b) has been adapted from ref [70] with permission from Wiley Online Library, copyright 2018. Panel (c) has been adapted from ref [71] with permission from Royal Society of Chemistry, copyright 2020.

mixing−irradiation−curing method. The rate of swelling and the color change depended on the alkyl chain length of the saturated aliphatic hydrocarbons. The mechanism of this color transition is complicated. The authors explained that the swelling of PDMS induced mechanical strain on the embedded PDA, which exposed the unreacted monomers present in the PDA crystals to the solvent and dissolved them, creating voids in the PDA structures. This combined effect of mechanical strain and void creation caused a decrease in interchain interactions in the PDA and served as a driving force for the PDA phase transition. The same group prepared a PDMS microbead–PDA composite sensor.[66] This sensor underwent a blue-to-red color change in response to the hydrocarbons of the shorter alkyl chains and enabled visual differentiation between n-pentane, n-heptane, n-nonane, and n-undecane (Figure 3b). The degree of swelling of the PDA–PDMS composite beads in these hydrocarbons was inversely correlated with the length of the alkyl chains.

Seo et al.[67] prepared a sensory system in which one-dimensional (1D) PDA nanofibers were integrated into the three-dimensional (3D) matrix of a hygroscopic alginate hydrogel to detect water (Figure 3c). Alginate has a dramatic volume swelling property when it absorbs water. This volumetric expansion induced mechanical stress on the PDA nanofibers, which deformed the PDA backbone, leading to the color transition.

2.7 Macroscopic scratch and rubbing

Chae et al.[69] prepared a directly writable crayon-like PDA–wax composite sensor by embedding different PDAs into paraffin wax (melting temperature 58–62 °C) (Figure 4a). The wax mixed with 2% PCDA showed irreversible thermochromism, whereas that with PCDA-mBzA presented a reversible color change. A mechanically drawn PDA image showed a colorimetric transition from blue to red upon heating or soft rubbing. Optical microscopy showed that diacetylene and the wax formed a complex at the single-crystal level, where the wax molecules intercalated between the diacetylene crystals. Upon heating, the PDA crystals underwent significant shrinkage because of the release of unreacted diacetylene monomers and embedded wax molecules from the crystal. The release of the wax molecules caused distortion of the arrayed p-orbitals and thus the blue-to-red color transition. The same group developed a reversible mechanochromic PDA by self-assembly of diphenyldisulfide-containing bisdiacetylene (PCDA-4APDS).[72] The temperature of the powder remained below the thermochromic

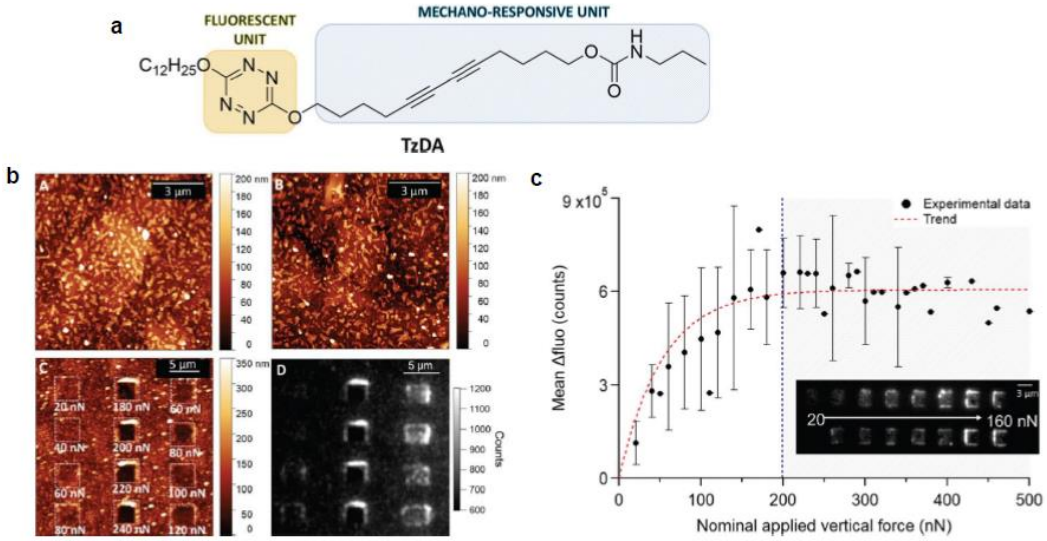

Figure 5: a, Schematic diagram of a molecular design of TzDA. **b,** AFM morphology images of the (A) monomer, (B) polymer, and (C) polymer after mechanical stimulation. (D) Fluorescence image of poly-TzDA after the application of various forces. **c,** Plot showing the recovered fluorescence signal vs. applied vertical force. This figure has been adapted from ref [48] with permission from Royal Society of Chemistry, copyright 2019.

transition temperature (80 °C) of the PDA during grinding, which proves that the color change was cause by the mechanical stress. The mechanical energy produced from grinding transferred to the alkyl chain of the PDA, which caused partial distortion of the conjugated ene–yne backbone, shortened the effective conjugation length of the PDA, and thus induced the color transition.

Ishijima et al.[73] prepared an organic-layered material using PDA with the intercalation of guest organic amines, that is, alkyl amines and alkyl diamines. The amine-intercalated PDA showed a tunable temperature (46–106 °C) and a mechanoresponsive color change. Rubbing gradually changed the PDA color, which indicated that force was the reason for the color change rather than heat during rubbing. The same group fabricated a paper-based friction detector based on the amine-intercalated PDA (Figure 4b).[70] The composite was formed through self-organization followed by polymerization, which was then homogeneously coated on a sheet of paper. The application of friction force by a cage showed a force-dependent color change with a detectable range of 7.6–23.0 N. The properties were tuned by using various types of guest ions and amines without complex synthesis. The measurement of writing pressure was demonstrated using a paper device. Weak, moderate, and strong writing forces in the range of 8.80–31.1 N were visualized and quantitatively detected by the friction force. The group further developed a layered PDA/PEI composite-coated paper device to detect weak force (Figure 4c).[71] In this work, tooth-brushing force in the range of 0.91–6.60 N was used as a model to create weak forces. Soft, normal, and hard brushing forces were applied to the paper-based PDA device, which showed the blue-to-red color change. Sparse modeling was used to analyze the PDA color images for selecting the best interlayer guest.

2.8 Atomic force microscopy

PDA studies by AFM were pioneered by Burns et al.[74] They observed an irreversible blue-to-red transformation by applying shear forces with an AFM tip. Out-of-plane rotations of the side chains caused by the tip–PDA interactions disrupted the π-orbital overlap, causing the mechanochromic transition. Although this work marked an important step toward PDA mechanochromism research at the nanoscale, the shear force used was shown only qualitatively as standard AFM can only quantify forces vertical to the substrate. The same group also prepared ultrathin PDA films using the horizontal Langmuir deposition technique from two diacetylene monomers, PCDA(I) and N-(2-ethanol)-10,12-pentacosadiynamide (PCEA) (II).[60] AFM or near-field scanning optical microscopy (NSOM) tips were used to apply qualitative shear forces. Their data revealed that the friction depended on the angle between the polymer backbone and the scanning direction; the maximum occurred when the scanning direction was perpendicular to the backbones. PCEA in particular exhibited threefold friction anisotropy depending on the scanning direction relative to the polymer backbone. These works revealed the anisotropic friction of PDA for the first time based on scanning microscopy.

Polachhi et al.[48] prepared a PDA derivative with an amplified fluorescence response by covalently linking a tetrazine fluorophore to diacetylene (poly-TzDA, Figure 5). The fluorescence emission wavelength from tetrazine matched with the absorption of blue PDA, causing an energy transfer only when the system was in the blue phase. Therefore, in the monomer state, the sample presented fluorescence from tetrazine, which was quenched during the polymerization owing to the increased amount of blue PDA.

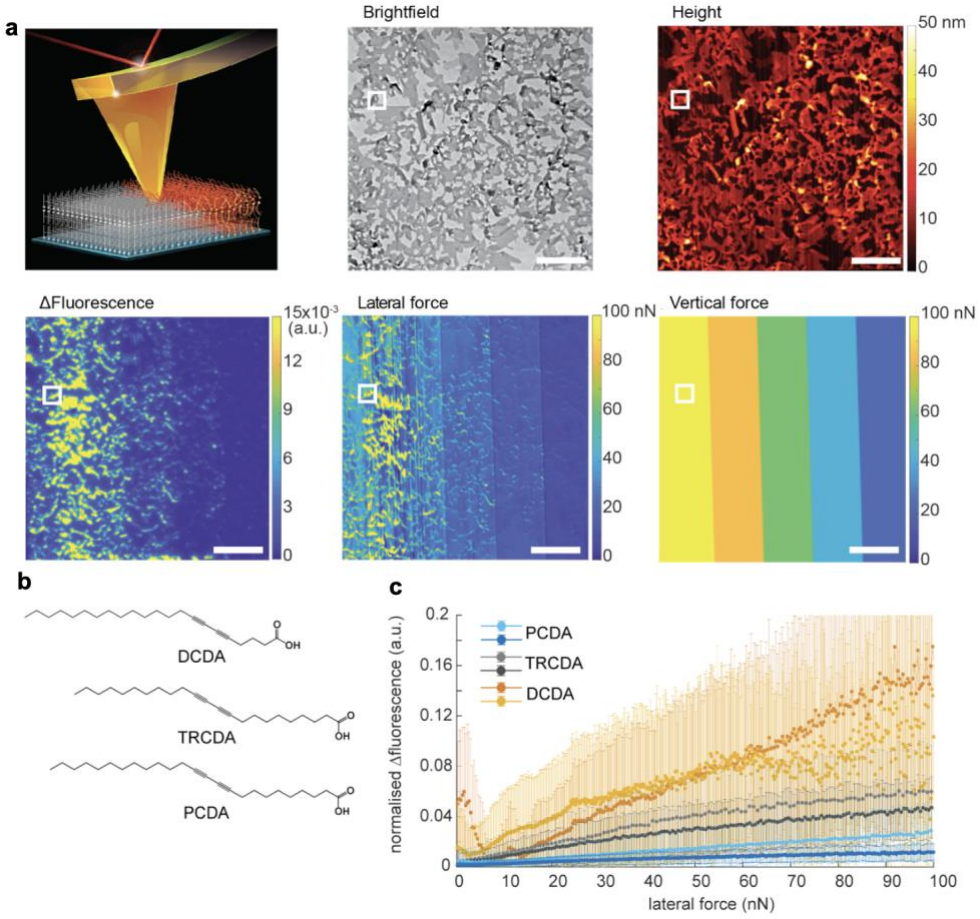

Figure 6: Characterization of 5,7-docosadiynoic acid (DCDA) Langmuir–Blodgett films by lateral force microscopy coupled with fluorescence microscopy. **a,** Scheme of the experiment, a bright-field microscopy image, an AFM height image, Δfluorescence before and after scratching, lateral force map, and vertical force map. The scale bars show 10 µm. **b,** Chemical structure of the used monomers with different color transition temperature (DCDA: 50 °C, TRCDA: 55 °C, PCDA: 65 °C). **c,** Fluorescence increase vs. lateral force. This figure has been adapted from ref [47] with permission from American Chemical Society, copyright 2021.

During the blue-to-red transition, the energy transfer was again weakened and the tetrazine fluorescence was efficiently restored. Poly-TzDA was further characterized using AFM coupled with fluorescence microscopy. A vertical force in the range of 20–500 nN was applied by the tip with a scanning speed of 6.1 µm s^{-1}. Fluorescence images showed that poly-TzDA restored its fluorescence emission locally from the scratched part of the film. Such a fluorescence resonance energy transfer (FRET)-based enhancement of PDA fluorescence may be used to improve its sensitivity toward sensing applications.

Although the abovementioned works showed that PDA is mechanochromic at the nanoscale and that shear force is the key to inducing the blue-to-red transition, they failed to quantify the shear forces required to activate PDAs. This is because standard AFM can measure and manipulate only the forces vertical to the substrate. In 2021, we overcame this bottleneck by utilizing quantitative friction force microscopy, which measures lateral forces (Figure 6).[47] Friction force microscopy is an AFM-based technique that enables the quantification of forces lateral to the substrate by calibrating lateral laser deflection into forces.[75, 76] The use of this experimental technique was partially enabled by our recent identification of an error source in the wedge calibration method over the nanonewton range.[77] Quantitative friction force microscopy combined with fluorescence microscopy confirmed that PDA reacts only to lateral forces, $F_{//}$, as the lateral force presents perfect correlation with Δfluorescence, whereas vertical force does not (Figure 6a). The setup also disproved the previously claimed hypothesis that the edges of the polymer crystals exhibit higher force sensitivity than the rest of the crystal. This was accomplished by correlating Δfluorescence and lateral forces at the edge and the bulk separately. In addition, we reported a link between mechanochromism and thermochromism, which can be attributed to the fact that both work and heat are different means of providing the same transition energy (Figure 6b, c).[47] These data provide the first insight into quantitative, anisotropic PDA mechanochromism at the nanoscale, where crystal-to-amorphous transition of PDA structure seems to play an important role. The friction force microscopy combined with fluorescence microscopy can be also used to characterize other mechanosensitive polymers[78-80] and mechanophores[81] in future.

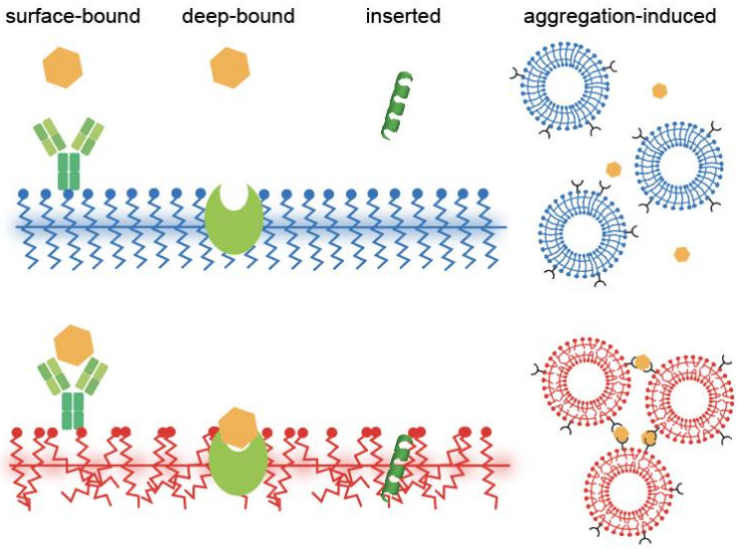

Figure 7: Categories of ligand-PDA interactions in biosensing.

3. Conclusions and future perspective

This minireview provides an overview of the recent progress in PDA mechanochromism, where various forces can be used as stimuli to induce the color change. The quantitative and anisotropic force–fluorescence correlation at the nanoscale obtained in recent years has just begun to provide a new perspective on its mechanism. In biosensing, bound ligands are expected to exert forces on PDAs, as in the case of an AFM cantilever, yet how each molecule does that is unclear in many cases. Ligands are often surface-bound,[82] deep-bound (where the receptor is embedded within PDAs),[83] inserted,[84] or aggregated[85] to initiate the color transition (Figure 7; also see the categorization shown in Table S1). Nevertheless, when binding to a receptor exposed on a PDA headgroup (surface-bound), there is no obvious reason why the ligand should apply force to the PDA except that some receptors undergo a conformational change after binding that induces stress on the PDA; alternatively, the ligands may eventually inserted into the PDA matrix, where the role of the binding was to elevate the local ligand concentration right above the PDA surfaces. Some binding events may not be interpreted as applying forces. For example, we previously reported that antimicrobial peptides are "partially melting PDAs" (inducing the solid-to-liquid phase transition of side chains) by increasing the disorder in the system, which turns their blue color to red.[61] In such a case, although the peptide–PDA mechanical interaction must occur, it is difficult to attribute a certain amount of force to the change in the color. As a future perspective, learning from the quantitative information obtained in mechanochromism studies and applying them in biosensing research to understand the detailed mechanism of how each ligand induces the color change will be useful for improving the sensitivity and selectivity, and thus for the further development of applications.

Author Contributions

K. S. has initiated the entire work and wrote the article together with B. D. The rest of S. J., J. Z., and J. C. all contributed to the literature search, the investigation of the current trends and making the Table S1 in SI.

Conflicts of interest

There are no conflicts to declare.

Acknowledgements

Part of the research leading to these results has received funding from Shiseido Female Researcher Science Grant, UTEC-UTokyo FSI Research Grant Program, the FY 2020 University of Tokyo Excellent Young Researcher, Japan Society for the Promotion of Science (JP20K22324), Takeda Science Foundation, the Mitsubishi Foundation, Inoue Foundation for Science, the Naito Foundation and the Kanamori Foundation.

Notes and references

1. Y. L. Tai and Z. G. Yang, *J Mater Chem B*, 2015, **3**, 5436-5441.
2. N. Hu, Y. Karube, M. Arai, T. Watanabe, C. Yan, Y. Li, Y. L. Liu and H. Fukunaga, *Carbon*, 2010, **48**, 680-687.
3. S. C. B. Mannsfeld, B. C. K. Tee, R. M. Stoltenberg, C. V. H. H. Chen, S. Barman, B. V. O. Muir, A. N. Sokolov, C. Reese and Z. N. Bao, *Nat Mater*, 2010, **9**, 859-864.

4. C. Ge and E. Cretu, *J Micromech Microeng*, 2017, **27**.
5. G. Wegner, *Zeitschrift für Naturforschung B*, 1969, **24**, 824-832.
6. O. Yarimaga, J. Jaworski, B. Yoon and J. M. Kim, *Chem Commun*, 2012, **48**, 2469-2485.
7. B. Yoon, S. Lee and J. M. Kim, *Chemical Society reviews*, 2009, **38**, 1958-1968.
8. R. Volinsky, S. Kolusheva, A. Berman and R. Jelinek, *Langmuir*, 2004, **20**, 11084-11091.
9. R. Volinsky, M. Kliger, T. Sheynis, S. Kolusheva and R. Jelinek, *Biosens. Bioelectron.*, 2007, **22**, 3247-3251.
10. Y. Tomioka, N. Tanaka and S. Imazeki, *J. Chem. Phys.*, 1989, **91**, 5694-5700.
11. C. Girard-Reydet, R. D. Ortuso, M. Tsemperouli and K. Sugihara, *J. Phys. Chem. B*, 2016, **120**, 3511-3515.
12. S. J. Kew and E. A. H. Hall, *Anal. Chem.*, 2006, **78**, 2231-2238.
13. R. A. Nallicheri and M. F. Rubner, *Macromolecules*, 1991, **24**, 517-525.
14. Q. Xu, S. Lee, Y. Cho, M. H. Kim, J. Bouffard and J. Yoon, *J. Am. Chem. Soc.*, 2013, **135**, 17751-17754.
15. S. Dolai, S. K. Bhunia, S. S. Beglaryan, S. Kolusheva, L. Zeiri and R. Jelinek, *Acs Appl Mater Inter*, 2017, **9**, 2891-2898.
16. X. Chen, L. Hong, X. You, Y. L. Wang, G. Zou, W. Su and Q. J. Zhang, *Chem Commun*, 2009, DOI: 10.1039/b820894h, 1356-1358.
17. X. Q. Chen, J. Lee, M. J. Jou, J. M. Kim and J. Yoon, *Chem Commun*, 2009, DOI: 10.1039/b904542b, 3434-3436.
18. Z. F. Ma, J. R. Li, M. H. Liu, J. Cao, Z. Y. Zou, J. Tu and L. Jiang, *J. Am. Chem. Soc.*, 1998, **120**, 12678-12679.
19. J. M. Kim, Y. B. Lee, D. H. Yang, J. S. Lee, G. S. Lee and D. J. Ahn, *J. Am. Chem. Soc.*, 2005, **127**, 17580-17581.
20. R. D. Ortuso, U. Cataldi and K. Sugihara, *Soft Matter*, 2017, **13**, 1728-1736.
21. S. Kolusheva, L. Boyer and R. Jelinek, *Nat. Biotechnol.*, 2000, **18**, 225-227.
22. L. L. Li, X. Q. An and X. J. Yan, *Colloid Surface B*, 2015, **134**, 235-239.
23. M. Ripoll, P. Neuberg, A. Kichler, N. Tounsi, A. Wagner and J. S. Remy, *Acs Appl Mater Inter*, 2016, **8**, 30665-30670.
24. E. Morin, M. Nothisen, A. Wagner and J. S. Remy, *Bioconjug. Chem.*, 2011, **22**, 1916-1923.
25. H. Jiang, X. Y. Hu, S. Schlesiger, M. Li, E. Zellermann, S. K. Knauer and C. Schmuck, *Angew Chem Int Edit*, 2017, **56**, 14526-14530.
26. V. Haridas, S. Sadanandan, P. Y. Collart-Dutilleul, S. Gronthos and N. H. Voelcker, *Biomacromolecules*, 2014, **15**, 582-590.
27. M. A. Desta, C. W. Liao and S. S. Sun, *Chem-Asian J*, 2017, **12**, 690-697.
28. J. Nishide, T. Oyamada, S. Akiyama, H. Sasabe and C. Adachi, *Adv Mater*, 2006, **18**, 3120-3124.
29. M. Ulaganathan, R. V. Hansen, N. Drayton, H. Hingorani, R. G. Kutty, H. Joshi, S. Sreejith, Z. Liu, J. L. Yang and Y. L. Zhao, *Acs Appl Mater Inter*, 2016, **8**, 32643-32648.
30. Y. K. Choi, H. J. Kim, S. R. Kim, Y. M. Cho and D. J. Ahn, *Macromolecules*, 2017, **50**, 3164-3170.
31. K. Morigaki, T. Baumgart, U. Jonas, A. Offenhausser and W. Knoll, *Langmuir*, 2002, **18**, 4082-4089.
32. J. Lee, H. Jun and J. Kim, *Adv Mater*, 2009, **21**, 3674-3677.
33. E. Y. Park, J. W. Kim, D. J. Ahn and J. M. Kim, *Macromol Rapid Comm*, 2007, **28**, 171-175.
34. H. O. Yoo, S. K. Chae, J. M. Kim and D. J. Ahn, *Macromol Res*, 2007, **15**, 478-481.
35. Y. Lifshitz, A. Upcher, O. Shusterman, B. Horovitz, A. Berman and Y. Golan, *PCCP*, 2010, **12**, 713-722.
36. H. Sixl, W. Neumann, R. Huber, V. Denner and E. Sigmund, *Phys Rev B*, 1985, **31**, 142-148.
37. Y. Lifshitz, Y. Golan, O. Konovalov and A. Berman, *Langmuir*, 2009, **25**, 4469-4477.
38. R. R. Chance and G. N. Patel, *Journal of Polymer Science: Polymer Physics Edition*, 1978, **16**, 859-881.
39. R. D. Ortuso, N. Ricardi, T. Bürgi, T. A. Wesolowski and K. Sugihara, *Spectrochim. Acta A Mol. Biomol. Spectrosc.*, 2019, **219**, 23-32.
40. P. E. Schoen and P. Yager, *Journal of Polymer Science: Polymer Physics Edition*, 1985, **23**, 2203-2216.
41. H. Tanaka, M. A. Gomez, A. E. Tonelli and M. Thakur, *Macromolecules*, 1989, **22**, 1208-1215.
42. Y. Okawa and M. Aono, *J. Phys. Chem.*, 2001, **115**, 2317-2322.
43. A. Burns, R. Carpick, D. Sasaki, J. Shelnutt and R. Haddad, *Tribology Letters*, 2001, **10**, 89-96.
44. R. W. Carpick, D. Y. Sasaki and A. R. Burns, *Langmuir*, 2000, **16**, 1270-1278.
45. Y. Okawa and M. Aono, *Surf. Sci.*, 2002, **514**, 41-47.
46. V. Dobrosavljević and R. M. Stratt, *Physical Review B*, 1987, **35**, 2781-2794.
47. L. Juhasz, R. D. Ortuso and K. Sugihara, *Nano Lett*, 2021, **21**, 543-549.
48. L. Polacchi, A. Brosseau, R. Metivier and C. Attain, *Chem Commun*, 2019, **55**, 14566-14569.
49. X. M. Sun, T. Chen, S. Q. Huang, L. Li and H. S. Peng, *Chemical Society reviews*, 2010, **39**, 4244-4257.
50. A. C. D. Pires, N. D. F. Soares, L. H. M. da Silva, N. J. de Andrade, M. F. A. Silveira and A. F. de Carvalho, *Food Bioprocess Tech*, 2010, **3**, 172-181.
51. J. P. Huo, Q. J. Deng, T. Fan, G. Z. He, X. H. Hu, X. X. Hong, H. Chen, S. H. Luo, Z. Y. Wang and D. C. Chen, *Polym Chem-Uk*, 2017, **8**, 7438-7445.
52. E. Lebegue, C. Farre, C. Jose, J. Saulnier, F. Lagarde, Y. Chevalier, C. Chaix and N. Jaffrezic-Renault, *Sensors-Basel*, 2018, **18**, 599.
53. J. T. Wen, J. M. Roper and H. Tsutsui, *Ind Eng Chem Res*, 2018, **57**, 9037-9053.
54. X. M. Qian and B. Stadler, *Chem Mater*, 2019, **31**, 1196-1222.
55. Z. J. Zhang, F. Wang and X. Q. Chen, *Chinese Chem Lett*, 2019, **30**, 1745-1757.
56. F. Fang, F. L. Meng and L. Luo, *Mater Chem Front*, 2020, **4**, 1089-1104.
57. M. Weston, A. D. Tjandra and R. Chandrawati, *Polym Chem-Uk*, 2020, **11**, 166-183.
58. Q. Huang, W. Wu, K. L. Ai and J. H. Liu, *Front Chem*, 2020, **8**, 565782.
59. E. Cho and S. Jung, *Molecules*, 2018, **23**, 107.
60. R. W. Carpick, D. Y. Sasaki, M. S. Marcus, M. A. Eriksson and A. R. Burns, *J Phys-Condens Mat*, 2004, **16**, R679-R697.
61. J. Nuck and K. Sugihara, *Macromolecules*, 2020, **53**, 6469-6475.
62. M. Nakamitsu, K. Oyama, H. Imai, S. Fujii and Y. Oaki, *Adv Mater*, 2021, **33**, 2008755.
63. H. B. Feng, J. Lu, J. H. Li, F. Tsow, E. Forzani and N. J. Tao, *Adv Mater*, 2013, **25**, 1729-1733.

64. M. Nakamitsu, K. Oyama, H. Imai, S. Fujii and Y. Oaki, *Adv Mater*, 2021, **33**.
65. D. H. Park, J. Hong, I. S. Park, C. W. Lee and J. M. Kim, *Adv Funct Mater*, 2014, **24**, 5186-5193.
66. J. Hong, D. H. Park, S. Baek, S. Song, C. W. Lee and J. M. Kim, *Acs Appl Mater Inter*, 2015, **7**, 8339-8343.
67. S. Seo, J. Lee, M. S. Kwon, D. Seo and J. Kim, *Acs Appl Mater Inter*, 2015, **7**, 20342-20348.
68. S. S. Lee, E. H. Chae, D. J. Ahn, K. H. Ahn and J. K. Yeo, *Korea-Aust Rheol J*, 2007, **19**, 43-47.
69. S. Chae, J. P. Lee and J. M. Kim, *Adv Funct Mater*, 2016, **26**, 1769-1776.
70. H. Terada, H. Imai and Y. Oaki, *Adv Mater*, 2018, **30**, 1801121.
71. K. Watanabe, H. Imai and Y. Oaki, *J Mater Chem C*, 2020, **8**, 1265-1272.
72. J. P. Lee, H. Hwang, S. Chae and J. M. Kim, *Chem Commun*, 2019, **55**, 9395-9398.
73. Y. Ishijima, H. Imai and Y. Oaki, *Chem-Us*, 2017, **3**, 509-521.
74. A. R. Burns, R. W. Carpick, D. Y. Sasaki, J. A. Shelnutt and R. Haddad, *Tribol Lett*, 2001, **10**, 89-96.
75. M. Varenberg, I. Etsion and G. Halperin, *Rev. Sci. Instrum.*, 2003, **74**, 3362-3367.
76. D. F. Ogletree, R. W. Carpick and M. Salmeron, *Rev. Sci. Instrum.*, 1996, **67**, 3298-3306.
77. R. D. Ortuso and K. Sugihara, *J Phys Chem C*, 2018, **122**, 11464-11474.
78. Q. Z. Yang, Z. Huang, T. J. Kucharski, D. Khvostichenko, J. Chen and R. Boulatov, *Nat Nanotechnol*, 2009, **4**, 302-306.
79. Y. J. Lin, H. R. Hansen, W. J. Brittain and S. L. Craig, *Journal of Physical Chemistry B*, 2019, **123**, 8492-8498.
80. K. L. Berkowski, S. L. Potisek, C. R. Hickenboth and J. S. Moore, *Macromolecules*, 2005, **38**, 8975-8978.
81. T. Seki, N. Tokodai, S. Omagari, T. Nakanishi, Y. Hasegawa, T. Iwasa, T. Taketsugu and H. Ito, *J Am Chem Soc*, 2017, **139**, 6514-6517.
82. Y. J. Zhang, B. L. Ma, Y. J. Li and J. H. Li, *Colloid Surface B*, 2004, **35**, 41-44.
83. S. Kolusheva, T. Shahal and R. Jelinek, *J. Am. Chem. Soc.*, 2000, **122**, 776-780.
84. S. Kolusheva, T. Shahal and R. Jelinek, *Biochemistry (Mosc).* 2000, **39**, 15851-15859.
85. R. R. Adhikary, O. Koppaka and R. Banerjee, *Nanoscale*, 2020, **12**, 8898-8908.